Modeling the 20 November 2003 Ionosphere Storm with GRACE

Seebany Datta-Barua, Todd Walter, Sam Pullen, and Per Enge
Stanford University

ABSTRACT

The Local Area Augmentation System (LAAS) provides differential GPS corrections for Category I precision approach to aviation users within tens of kilometers of the LAAS Ground Facility (LGF). To ensure integrity, any circumstance that may lead to hazardously misleading information (HMI) being transmitted to the user must be identified. If the probability of the situation exceeds the allocated integrity risk, its maximum user errors must be bounded by one or more user-computed protection levels. Over short baselines, the differential ionosphere error between a user and LGF can pose one such threat.

This work examines how the spatial rate of change of the ionosphere over baselines of tens of kilometers can be modeled to provide insight into hazardous conditions. We develop a static spatial model of the ionosphere based on a technique developed for understanding the impact on WAAS of the 31 October 2003 localized nighttime ionosphere enhancement. In this work we apply the method to the 20 November 2003 ionosphere storm, a day on which GPS observations of the disturbed ionosphere were previously used to populate the space of possible ionosphere threats to LAAS users.

This 3-D model assigns vertical profiles to latitude and longitude regions. The horizontal "enhancement" and "background" ionosphere regions are identified based on measurements made by the Continuously Operating Reference Stations (CORS). Since observations of vertical density variations are limited with GPS receivers on the ground, space-based GPS data from on board one of the GRACE satellites passing through the disturbed ionosphere around 19:40 UT is used to test a range of vertical electron density profiles. The 500 km orbital altitude of the GRACE satellites effectively limits the contribution to the total electron content of the topside and plasmasphere. After finding the electron density model that minimizes the mean squared error, we then integrate through the lines of sight of a set of CORS receivers located in Ohio and separated by baselines as short as 50-75 km. Pairs of these stations mimic user-LGF pairs and were used in the literature to estimate the possible spatial decorrelation over LAAS baselines. We integrate through the CORS lines of sight (LOS) to compute the differential ionosphere over tens-of-kilometer baselines.

We find that a 3-D static model of the ionosphere cannot reproduce the 350-400 mm/km spatial rates of change in ionosphere error that have been verified with data. However, we find that allowing the ionosphere anomaly to sweep westward at 300 m/s, as has been estimated from data, can in fact reproduce rates of change between neighboring CORS stations on the order of 400 mm/km. Further refinements are needed to optimize the model-predicted delay over the three-hour timespan of the terrestrial observations, though the gross features are similar. This work confirms that the relative velocity of the ionosphere structure and the lines of sight are an important factor in apparent gradients in the ionosphere and also helps to further validate the estimates made from the CORS observations of short baseline spatial rates of change in ionosphere delay.

INTRODUCTION

The Federal Aviation Administration's Local Area Augmentation System (LAAS) is a Ground-Based Augmentation System (GBAS) designed to provide differential GPS corrections to users within tens of kilometers of a single airport [6]. LAAS must meet the demands in accuracy, availability, and integrity needed for Category II/III landings. The LAAS architecture consists of the LAAS Ground Facility (LGF), which is a reference location equipped with four dual-frequency GPS receivers typically placed near the runway. As a DGPS system it broadcasts ionosphere corrections and bounds to the user via a VHF data broadcast (VDB).

Bounds must be placed on the difference in ionospheric errors between an incoming aircraft and the LGF with minimal loss in availability. The ionosphere delay at a receiver is proportional to the total electron content (TEC), the integral of the electron density along the signal raypath. Because the ionosphere typically varies smoothly for a user and LGF separated by only a few kilometers, the nominal ionospheric error correction broadcast is 2-5 mm of delay difference per km of user-LGF separation distance [11]. However, to ensure user safety, what matters is not the typical so much as the near-worst-case ionosphere conditions. Such circumstances occurred on 20 November 2003.

During this event a coronal mass ejection from the sun arrived at the earth and caused extremely stormy behavior in the ionosphere. In the North American sector a large storm-enhanced density (SED) with equivalent vertical delays greater than 20 m developed over the southern Conterminous U.S. (CONUS) in the daytime. A long, narrow filament of enhanced electron density stretching from the SED northwest toward the magnetic pole was also observed. Foster et al. suggested this large "tongue of ionization" (TOI) was created by electric fields effectively channeling electrons poleward and that it was connected with plasmasphere erosion [7]. This TOI region is of interest for the LAAS ionosphere threat model because observations of some of the highest recorded spatial rates of change over short baselines were made during its passage over the midwestern US [4].

Extensive work has been done by Luo et al. in developing and parameterizing a threat model to represent it [12] and [13]. The anomalous ionosphere was modeled by a linear spatial rate of change of ionosphere error, a horizontal distance over which the spatial rate of change occurs, a ground speed of the anomaly, and the elevation at which the anomalous ionosphere is viewed. Ene et al. used data to characterize and validate events that have been observed to occur within this parameter space [5]. Lee et al. ran simulations to quantify the impact of the boundaries of this parameter space on LAAS Cat I availability [10]. More recently, Park et al. have run a LAAS-like differential GPS corrections between a pseudo-user/LGF pair of stations to confirm that the vertical position error could in fact be many meters beyond the vertical protection level, and therefore that the conservatism built into the threat model is justified [15].

The goal of this paper is to use ground station GPS data over CONUS and space-borne GPS data to develop a spatial model of the electron density that is consistent with the spatial decorrelation rates of 400 mm/km verified in the literature. We use the ground-based CORS GPS network and the GRACE satellites with their onboard GPS receivers. The terrestrial data are used to develop a density field that is piecewise continuous horizontally between the SED, TOI, and background regions. In each region of the model, we assign a possible vertical electron density profile. We integrate through the space-based GRACE GPS receiver lines of sight to find the choice of density profiles that minimizes the mean squared error. With this three-dimensional model, we then integrate through the lines of sight in a region of CORS with a high density of stations to predict possible spatial gradients. In the last section we will show that a 3-D electron density model cannot produce the gradients on the order of 400 mm/km that have been observed. On the other hand, we provide evidence that, by allowing for a time variation of the ionosphere by sweeping the TOI westward at 300 m/s, a simple 4-D extension of the model can in fact predict gradients of hundreds of mm of differential delay per km of receiver separation distance.

DATA

The Continuously Operating Reference Stations (CORS) are a network of almost 400 GPS receivers in the U.S. whose data are made publicly available in the Receiver INdependent EXchange (RINEX) format by the National Geodetic Survey [16]. The CORS sites considered in particular in this work are dual-frequency GPS receivers operated by the Ohio Department of Transportation [14]. The observations from these stations made during the 20 November 2003 storm have been assimilated and leveled by the use of the Global Ionospheric Mapping (GIM) software at NASA's Jet Propulsion Laboratory (JPL). With the additional use of the publicly available International GNSS Service station data worldwide, GIM estimates and removes satellite and receiver interfrequency biases to provide high precision ionosphere measurements. The processing is described in detail by Komjathy et al. [9]. The data are provided at 5-minute intervals.

The Gravity Recovery and Climate Experiment (GRACE) is a NASA and DLR (Germany) science mission satellite system established to measure variations in earth's gravity field [1]. The system consists of two satellites in a near-polar orbit at 500 km altitude in the same orbital plane 220 km apart. Dual-frequency Blackjack GPS receivers developed at JPL are used for precise orbit determination and atmospheric occultation on each [18]. The GPS data from each of the two satellites is made publicly available for download in RINEX format.

A map of the equivalent vertical delay assuming a 350 km ionosphere shell height over the eastern U.S. based on dual frequency CORS measurements on 20 November 2003 at 19:38 UT are plotted in Figure 1. The color at each point on the map corresponds to the ionosphere delay

at GPS L1 frequency, in meters from 0 (blue) to 20 (red). Figure 1a shows the ground track of the GRACE lead satellite "A" from 19:33–19:43 UT in black as it travels from south to north, and Figure 1b shows the same for GRACE-B. The satellites' positions at 19:36:30, 19:38:00, and 19:39:00 UT are marked with a square, triangle, and circle, respectively. From 19:33-19:43 UT GRACE-A and -B tracked several GPS satellites. Shadowed broken line segments point from the position of each GRACE satellite at 19:38 UT toward the GPS satellites identified by their PRN numbers: 1, 2, 3, 7, 8, 11, 13, 27, 28, and 31. Shorter line segments point toward higher elevation satellites.

The map of delays over the eastern U.S. show the storm-enhanced density (SED) region over the southeast, Gulf of Mexico, and mid-Atlantic. Also prominent is the tongue of ionization (TOI) extending from the SED northwest over Virginia, through Ohio, and beyond. The timing of the GRACE orbit is so fortuitous that it passes through the TOI as well as the SED during these few minutes.

With code measurements ρ_1 and ρ_2 and carrier phase measurements ϕ_1 and ϕ_2 at the two frequencies L1 and L2, the slant ionosphere delay I_s can be estimated directly from the GRACE GPS receivers. The dual frequency estimate of the ionosphere is formed from the GPS observables as

$$
\begin{aligned}
I_\rho &= \frac{\rho_2 - \rho_1}{\gamma - 1} && (1)\\
&= I_s + \frac{\gamma}{\gamma - 1}(IFB + \tau_{gd}) && (2)\\
&\quad + \frac{1}{\gamma - 1}(\epsilon_{\rho_2} - \epsilon_{\rho_1}) && (3)\\
I_\phi &= \frac{\phi_1 - \phi_2}{\gamma - 1} && (4)\\
&= I_s + \frac{\gamma}{\gamma - 1}(IFB + \tau_{gd}) && (5)\\
&\quad - \frac{1}{\gamma - 1}(N_2\lambda_2 - N_1\lambda_1) && (6)\\
&\quad - \frac{1}{\gamma - 1}(\epsilon_{\phi_2} - \epsilon_{\phi_1}) && (7)
\end{aligned}
$$

The estimate of the ionosphere formed from the code phase does not contain the unknown integer number of cycles at L1 N_1 and at L2 N_2, but it is noisy because $\epsilon_{\rho_i} >> \epsilon_{\phi_i}$. Both estimates I_ρ and I_ϕ contain the satellite hardware bias τ_{gd} and receiver interfrequency bias IFB. The GRACE slant TEC measurements I_s are formed from the GPS dual frequency code and carrier measurements I_ρ and I_ϕ with the broadcast satellite bias, receiver interfrequency bias, and integer ambiguities estimated and removed such that the background delay outside of the TOI and SED regions is only a couple meters.

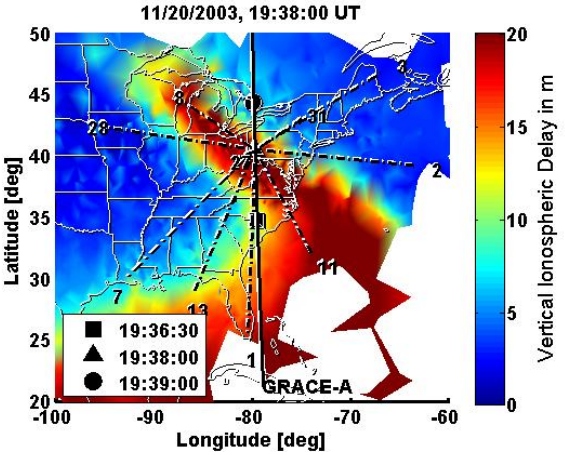

(a) GRACE-A

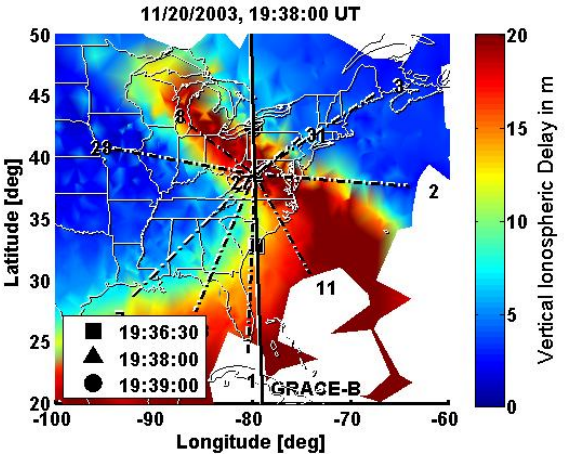

(b) GRACE-B

Fig. 1: Map of ionosphere vertical delay based on CORS data and GRACE satellites' ground track. Line segments point toward GPS PRNs' positions at 19:38 UT.

The ionosphere slant delay at L1 frequency from 19:33–19:43 UT for GRACE-A and -B are shown in the upper and lower plots, respectively, of Figure 2. The times 19:36:30, 19:38:00, and 19:39:00 UT are marked by vertical lines with squares, triangles, and circles, respectively, at the endpoints. The position of GRACE at these times are denoted with the corresponding symbol on the TEC map in Figure 1. Data for a line of sight below 0 degree elevation are not plotted. These lines of sight below the GRACE orbit altitude would graze through the ionosphere twice. For clarity, we choose to consider only upward lines of sight. The data during which cycle slips were detected, e.g.from 19:39–19:43 UT for PRN 28 (red dashed line), were removed.

The slant delays begin at 10 - 50 m, depending on the line of sight. As the GRACE satellites travel north through the SED, the delays tend to decrease. The exception is the

southward line of sight (LOS) to PRN 1 (dashed blue line), whose delay holds steady at about 38 m for the first three minutes. By 19:36:30 UT, most of the LOSs have dropped to a local minimum delay around 5 - 10 m. The exceptions are PRNs 2 and 3 to the east and northeast, whose delays reach an inflection point but are upwards of 15 m. For GRACE-A, PRNs 1 and 7 to the south and southwest also have delays greater than 15 m. In contrast PRN 13, which is also to the southwest (see Figure 1) does not have delays as high as PRNs 1 and 7. For GRACE-A most of the slant delays start to rise again after 19:36:30 UT, peaking at 20–40 m two minutes later as the satellite passes through the TOI, and then fall again to quiet 0 - 5 m delays. The delay peak due to the TOI is not quite symmetric; the falling edge is very slightly steeper than the rising edge. The LOS looking southwest at low elevation to PRN 13 does not drop, but remains at 25 m delay before the GPS satellite sets below 0 degree elevation at 19:42 UT. For GRACE-B a similar pattern of passage through the SED followed by the TOI occurs, offset by about 30 s. In the remaining sections we focus on only the GRACE-A measurements.

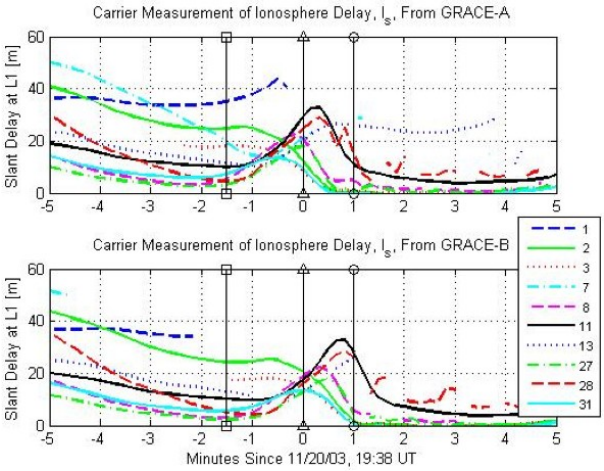

Fig. 2: Dual-frequency code-leveled carrier phase GPS measurements of slant ionosphere delay at L1 from GRACE-A (upper plot) and GRACE-B receivers from 19:33-19:43 UT.

THREE-DIMENSIONAL DENSITY MODEL

In this section we build a model of the electron density of the TOI, SED, and background regions that then can reproduce the observations of the GRACE-A satellite. The technique is two identify three regions horizontally – the TOI enhancement, the SED enhancement, and the background – based on the CORS ground network data. We identify latitude and longitude boundaries to these regions and assign each of the regions a vertical electron density profile. Then, knowing the position of GRACE-A and the GPS satellites, we integrate the electron density through the straight line raypath between them to compute the total electron content. This is the model prediction of the ionosphere delays that GRACE-A would experience. The cartoon in Figure 3 illustrates this method for one enhancement region and one LOS.

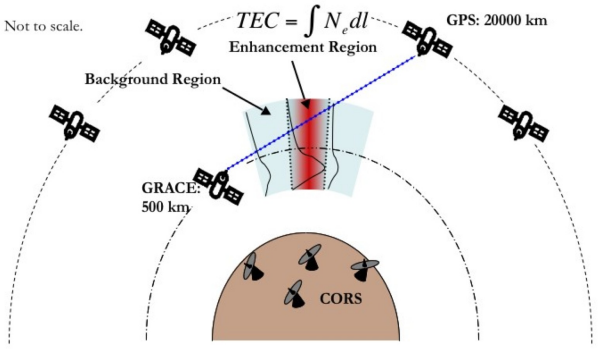

Fig. 3: Illustration of three-dimensional electron density modeling technique. Figure not to scale.

We define each CORS measurement to be within the enhancement or not based on whether the magnitude of its equivalent vertical delay at 350 km shell height is greater than a threshold of 12 m. Then, for a given choice of altitude, the convex hull formed from the ionosphere pierce points (IPPs) whose measurements were defined to be inside the enhancement has a certain area. As the altitude increases, the area decreases, reaches a minimum, then increases again. Effectively, the enhancement region "comes into focus" at the altitude where the area is minimum and then "goes out of focus" as the altitude continues to increase. By minimizing the area we hope to produce the high spatial rates of change of the ionosphere with the model that were observed in the data. To distinguish between the SED and the TOI enhancements, we enforce a boundary at 35 degrees north latitude. The map in Figure 4 shows the SED and TOI regions colored black and outlined in white. For the TOI region, we define a center line running NNW-SSE that represents the axis through the centroid. For the SED, we define a center line running WNW-ESE through the centroid. These axes are depicted in white in Figure 4, and neglect earth-curvature effects. Recalling the asymmetry of the GRACE measurements through the TOI, we shift its center line east one degree of longitude from the position shown in Figure 4.

At each point of latitude and longitude, we assign a vertical electron density profile. For the background region, this electron density profile is based on the International Reference Ionosphere (IRI) 2000 model. The IRI model is a global climatological model that produces electron density profiles for a specified place and time [2]. Since the enhancement regions are not predicted by the IRI model alone, we test a range of Chapman functions. The Chapman

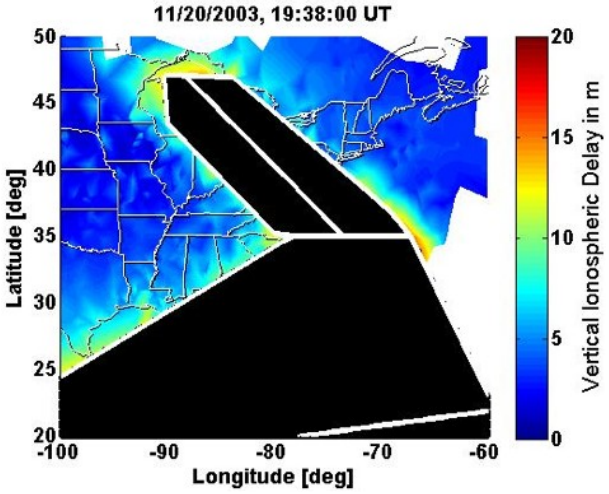

Fig. 4: Map of ionosphere with TOI region and SED region in black. The boundaries of these regions are outlined in white, as is the center line of each region.

function is a physics-based density profile based on equilibrium between the sun's ionizing radiation from above and recombination with ions, which increases at lower altitude [17]. The form of the function is:

$$f(h) = N_{e,max} exp\left(1 + \frac{h_{mF2} - h}{H} - e^{\frac{h_{mF2}-h}{H}}\right) \quad (8)$$

In Equation 8, the electron density varies with height h above the surface of the earth. The parameter $N_{e,max}$ is the maximum electron density and h_{mF2} is the altitude at which the maximum density occurs. The parameter H is the scale height, which effectively determines the width of the peak [8]. The Chapman function is defined up to a height of 1100 km, which is the altitude at which the plasmasphere typically dominates.

One Chapman function is assigned to points along the center line of the TOI, and one assigned to the center line of the SED. A linear combination of the Chapman function and the background profile is assigned to each point within the enhancement region, scaled by the distance, perpendicular to the center line, from that point to the boundary.

First holding the Chapman parameters for the SED fixed, we assign the three parameters $N_{e,max}$, h_{mF2}, and H a range of values for the TOI. The peak height varies from 200 to 800 km and the scale height from 50 to 250 km. The values for $N_{e,max}$ are given in MKS units by:

$$N_{e,max} = \frac{4\pi^2 f_{0F2} m_e \epsilon_0}{e^2} \quad (9)$$

$$f_{0F2} = 10, 12, 14, ...20 \quad MHz \quad (10)$$

In these expressions the critical frequency f_{0F2} is the minimum frequency wave that will propagate through the ionosphere, m_e is the mass of the election, ϵ_0 the permittivity of free space, and e is the charge of the electron.

The predicted TEC from the GRACE-A satellite to a GPS satellite is the sum of the electron densities at each point along the raypath. For each choice of parameters, we difference the predicted TEC from the measurements shown in Figure 2a and compute the mean squared error (MSE). The MSE as a function of peak height h_{mF2} and scale height H is shown in Figure 5. Each mesh surface corresponds to a single choice of $N_{e,max}$, as given by Equation 9. The z-axis and the color both correspond to the log of the MSE.

Each of the surfaces reaches a minimum at scale height $H = 250$ km, and the minimum MSE is nearly the same for all values of $N_{e,max}$. As $N_{e,max}$ increases, the peak height h_{mF2} at which this minimum MSE occurs decreases. The choice of parameters for which the MSE is minimized is (h_{mF2}, H, f_{0F2}) = (450 km, 250 km, 14 MHz), but it is a shallow minimum. Similarly holding this function fixed for the TOI and allowing the Chapman parameters to vary for the SED, we find the MSE minimized at (h_{mF2}, H, f_{0F2}) = (550 km, 50 km, 20 MHz), but this also is a shallow minimum. The same inverse relationship between peak density $N_{e,max}$ and peak height h_{mF2} holds. This is to be expected since our ground measurements are fairly insensitive to vertical electron density variations, and the number of GRACE-A measurements, though they improve observability vertically, are so limited.

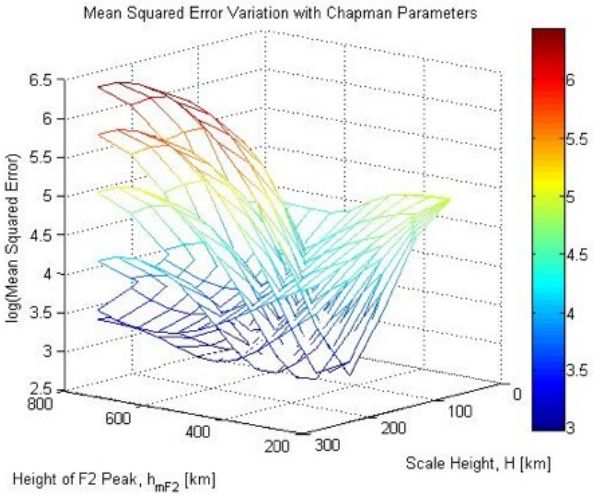

Fig. 5: Mean squared error between model prediction and GRACE-A measurements as a function of hmf2 and H. Each surface corresponds to Nemax for fof2 = 10,12,14,16,18,20 MHz.

To compare our model to the actual measurements, we replot the GRACE-A satellite measurements to GPS satellites above 0 degrees elevation in Figure 6a. Using the electron density field specified for the TOI, SED, and background regions so as to minimize the MSE as described above, we plot in Figure 6b the slant ionosphere delays predicted by the model for the same lines of sight.

The model recreates the same general features seen in the data. The slant delays begin at 15-50 m, depending on the LOS, decreasing until 19:36:30 UT. After this the delays increase until they peak right around 19:38:00 UT as they travel through the TOI, and decrease to the background few meter level. The amplitudes of the TOI peaks for PRNs 11 (black line) and 28 (dashed red lines) are slightly low, and for PRN 7 the minimum between the SED and TOI is about 5 m too high.

The most noticeable discrepancy between the measurement and model occurs for PRN 2 (green line). The SED delay at 19:33 UT is about 7 m too low and drops so that the local minimum between the SED and TOI is about 15 m lower than the true measurements. This is most likely due to the fact that the LOS is to the east over the Atlantic. In this direction the uncertainty in our data-based model increases because there are few measurements and no CORS ground stations located in the Atlantic. This may not be the sole explanation, though, since PRNs 3 (dotted red line) and 11 (black line) are to the northeast and southeast respectively, and the model agrees with the measurements to within a few meters for these LOSs.

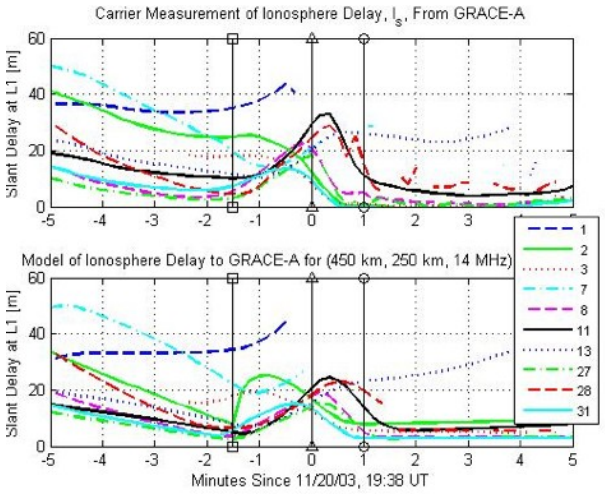

Fig. 6: GRACE-A measurements (top) and model that gives minimum mean squared error (bottom) as a function of time. For this model, the Chapman function for the TOI was hmf2 = 450 km, H - 250 km, and fof2 = 14 MHz.

SPATIAL DECORRELATION FROM MODEL

We developed a static three-dimensional electron density model based on both ground- and space-based data for the 20 November 2003 electron enhancement over the U.S. in the previous section. Here, we compute the model's predictions of the ground measurements observed from the Ohio CORS stations. Recall that many of the largest spatial rates of change, on the order of 350-400 mm of differential delay per km of receiver separation, were observed from these stations [5]. A map of these stations is shown in Figure 7. The nearest stations are separated by 50-75 km.

As an example of the Ohio CORS observations, Figure 8a shows the JPL-processed, dual-frequency CORS measurements from six stations in Ohio to PRN 28 from 18:50–21:50 UT. This is a three-hour time span, unlike the ten-minute time window considered for GRACE. Vertical line segments at 19:40, 20:20, and 21:00 UT are marked with a square, triangle, and circle respectively at the endpoints. The vertical bar at 19:40 UT corresponds most closely to the time during which the GRACE data were considered above. The delays begin at the couple meter level and rise from 19:50 UT to reach 30–40 m. The peak is reached by 20:30 UT for the easternmost station GARF. Peaks are reached according to receiver location, from northeast to southwest. After this time, the delays fall quickly for ten minutes, reach a plateau rising slowly for almost twenty minutes and then drop rapidly to the background value of a couple meters. This also happens sequentially to the stations from northeast to southwest. In several cases the final drop happens so rapidly that the data were most likely screened out by the cycle-slip-detection stage of processing [9].

In contrast, the predictions of the three-dimensional electron density model developed above are plotted for each LOS to PRN 28 in Figure 8b. The background value begins at 20 m rather than 3-4 m. The TOI peak reaches a reasonable value of 35 m, but this is only 15 m higher than the background. The peaks occur at each station in the same northeast-southwest sequence. However, the timing of the peaks are delayed by tens of minutes with respect to the actual measurements.

We difference simultaneous delays between each pair of stations, and divide the differential delay by distance between the pair of stations to compute the spatial decorrelation predicted by this 3-D model. A histogram of these rates of change is shown in Figure 9. Previous studies showed 350–400 mm/km [3], but the outliers on the histogram resulting from our model only lie in the 80–100 mm/km rate of change. While still anomalous, this is lower than the worst case observations of the storm from this location at this time by a factor of 3 or 4.

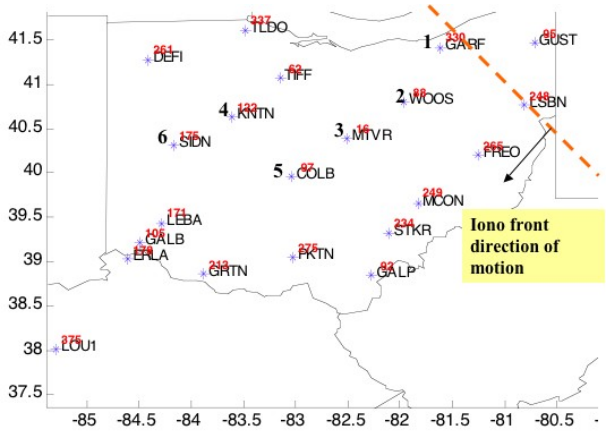

Fig. 7: Map of CORS stations in Ohio with site IDs (letters) and receiver number in the CORS data set (red). Numbers in black show the sequence in which the measurements to PRN 28 peak in Figure 8a.

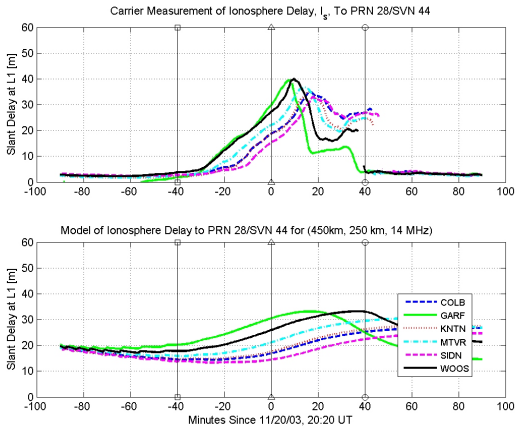

Fig. 8: Ohio CORS station measurements (top) and model (bottom) that gives minimum mean squared error with GRACE-A as a function of minutes since 20:20 UT. For this model, the Chapman function was h_{mF2} = 450 km, H = 250 km, and f_{0F2} = 14 MHz, and the TOI boundary was fixed with respect to the ground.

It is very likely that this discrepancy in the magnitude of the decorrelation lies in the fact that, over the 10-minute time window that GRACE passed through the feature, the assumption of a static ionosphere was reasonable. In contrast, the duration of the TOI passage over the Ohio CORS stations is over an hour. Also, estimates of the ground speed of the ionosphere anomaly have been 200–300 m/s for this feature [5]. These speeds are comparable to the speeds of the ionosphere pierce points (IPPs) of the lines of sight from the ground station.

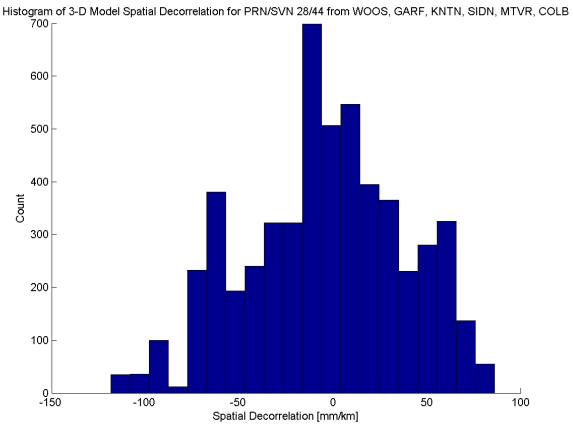

Fig. 9: Histogram of spatial decorrelation between pairs of six Ohio CORS stations. The outliers reach 80-100 mm/km for a ground-fixed TOI.

To test whether this can account for the differences between Figure 8a and 8b, we extend the 3-D density model into an extremely simple 4-D model. The TOI is now made to sweep westward at 300 m/s such that at 20:20 UT it reaches the position at which it was modeled above. Assigning to each point along each raypath a density according to its position within either the moving TOI, stationary SED, or background, we integrate to compute the delay for each LOS between the same Ohio stations and PRN 28 as before. The prediction of this four-dimensional model is plotted in Figure 10b, below the CORS measurements replotted in 10a.

As with the 3-D model, the background delays begin too high at 20 m. They drop to within 5 m of the measured values by 19:50 UT. At this time, each LOS's delay rises in the correct sequence at about the correct rate in time. The delay peaks for GARF at 40 m, as the measurements do, but happens about 10 minutes early. The remaining LOSs peak and decline gradually in the correct sequence for about 20 minutes. Then each drops rapidly to the background value of 10 m, again sequentially from northeast to southwest.

Our model extended to four dimensions in this simple way does not capture the detailed local minimum structure after 20:40 UT in the measurements in Figure 10a. The ionosphere structures are no likelier to travel at constant 300 m/s speed for three hours than they are to remain perfectly ground-fixed over that time. Nevertheless, the amplitude and the time rates of change are much more akin to those of the measurements. The TOI appears to pass through the lines of sight for a time period of close to one hour, much as the measurements do. Differencing the delays between pairs of the six stations and dividing by the distance between the stations, we compute the spatial decorrelation in

mm of delay at L1 frequency per km of receiver separation. A histogram of these spatial rates are shown in Figure 11. The outliers are the points of interest, and they occur in the 350–400 mm/km range. This is the approximate magnitude at which spatial decorrelation rates between these pairs of stations have been estimated with the data.

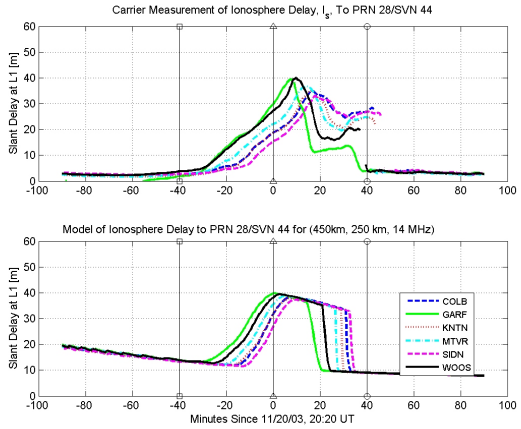

Fig. 10: Ohio CORS station measurements (top) and model (bottom) that gives minimum mean squared error with GRACE-A as a function of minutes since 20:20 UT. For this model, the Chapman function had h_{mF2} = 450 km, H = 250 km, f_{0F2} = 14 MHz, and the TOI boundary shifted westward at 300 m/s.

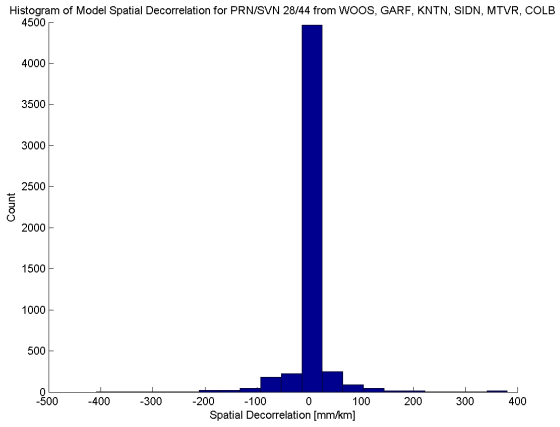

Fig. 11: Histogram of spatial decorrelation between pairs of six Ohio CORS stations. The outliers reach 350-400 mm/km for a TOI moving west at 300 m/s.

CONCLUSION

Our aim in this work was to apply a technique developed for WAAS for modeling anomalous ionosphere structures to an event of particular interest for the FAA LAAS program. We modeled the 20 November 2003 electron density over the U.S. during local afternoon as a first step in further validating the parameters of the LAAS threat model. This model used data from the CORS network of stations to identify latitude and longitude boundaries to ionosphere structures. We used space-based GPS data from one of the GRACE satellites to provide some observability of the altitude variation to refine our choice of vertical density profiles. We found that the region known as a "tongue of ionization" (TOI) extending northwest across the U.S. could be modeled with a thickened peak region whose scale height was around 250 km. The peak height and critical frequency were not as well distinguished by minimizing the mean square error between model and GRACE-A measurements. In comparing this model to lines of sight from GPS to the ground, our preliminary finding is that the ionosphere structure velocity is a key element in modeling storm-time effects on ground receivers. Allowing for nonzero TOI speed produced spatial decorrelation rates as high as 350–400 mm/km. We feel this model is reasonably consistent with observations that have been confirmed in the literature and included in the LAAS threat model.

ACKNOWLEDGMENTS

The authors would like to thank the FAA Wide Area Augmentation System Program Office for supporting this research. The efforts of Attila Komjathy at JPL in processing the CORS network data are appreciated. Thanks to Godwin Zhang for providing the map of the Ohio CORS stations.

REFERENCES

[1] D. Adam. Gravity measurement: Amazing grace. *Nature*, 416(6876):10–11, 2002.

[2] D. Bilitza. International reference ionosphere 2000. *Radio Science*, 36(2):261–275, March/April 2001.

[3] T. Dehel. Suspected relationship of tec change in a 'trough-like depletion' with prior measurements of o+ outflow. private correspondence, May 16 2005.

[4] T. F. Dehel. Observations of ionospheric walls of tec during geomagnetic storms. In *Proceedings of the Institute of Navigation Annual Meeting*, pages 264–299, 2005.

[5] A. Ene, D. Qiu, M. Luo, S. Pullen, and P. Enge. A comprehensive ionosphere storm data analysis method to support laas threat model development. In *Proceedings of the Institute of Navigation National Technical Meeting*, pages 110–130, 2005.

[6] P. Enge. Local area augmentation of gps for the precision approach of aircraft. *Proceedings of the IEEE*, 87(1):111–132, January 1999.

[7] J. C. Foster, A. J. Coster, P. J. Erickson, J. M. Holt, F. D. Lind, W. Rideout, M. McCready, A. van Eyken,

R. J. Barnes, R. A. Greenwald, and F. J. Rich. Multiradar observations of the polar tongue of ionization. *Journal of Geophysical Research*, 110(A9, A09S31), 03 September 2005.

[8] A. J. Hansen. *Tomographic Estimation of the Ionosphere Using Terrestrial GPS Sensors*. PhD thesis, Stanford University, March 2002.

[9] A. Komjathy. Automated daily processing of more than 1000 ground-based gps receivers for studying intense ionospheric storms. *Radio Science*, 40(RS6006), 2005.

[10] J. Lee, M. Luo, S. Pullen, Y. S. Park, P. Enge, and M. Brenner. Position-domain geometry screening to maximize laas availability in the presence of ionosphere anomalies. In *Proceedings of the Institute of Navigation GNSS Meeting*, pages 393–408, 2006.

[11] J. Lee, S. Pullen, S. Datta-Barua, and P. Enge. Assessment of nominal ionosphere spatial decorrelation for laas. In *Proceedings of the Position Location and Navigation Symposium*. Institute of Navigation/ Institute of Electronics and Electrical Engineers, 2006.

[12] M. Luo, S. Pullen, A. Ene, D. Qiu, T. Walter, and P. Enge. Ionosphere threat to laas: Updated model, user impact, and mitigations. In *Proceedings of the Institute of Navigation GNSS Meeting*, pages 2771–2785, 2004.

[13] M. Luo, S. Pullen, T. Walter, and P. Enge. Ionosphere spatial gradient threat for laas: Mitigation and tolerable threat space. In *Proceedings of the Institute of Navigation National Technical Meeting*, pages 490–501, 2004.

[14] S. McGowan. Ohio dot's vrs network. *Professional Surveyor Magazine*, 24(12):8,9,12,14, December 2004.

[15] Y. S. Park, J. Lee, M. Luo, S. Pullen, and P. Enge. Data-replay analysis of laas safety during ionosphere storms. In *Proceedings of the Institute of Navigation GNSS Meeting*, 2007. in publication.

[16] R. A. Snay. The national and cooperative cors systems in 2000 and beyond. In *Proceedings of the Institute of Navigation GPS Meeting*, pages 55–58, 2000.

[17] T. F. Tascione. *Introduction to the Space Environment*. Krieger Publishing Company, Malabar, Florida, 1994.

[18] J. Wickert, G. Beyerle, R. Konig, S. Heise, L. Grunwaldt, G. Michalak, C. Reigber, and T. Schmidt. Gps radio occultation with champ and grace: A first look at a new and promising satellite configuration for global atmospheric sounding. *Annales Geophysicae*, 23(3):653–658, 2005.